

HIGH ORDER DISCONTINUOUS FINITE-VOLUME/FINITE-ELEMENT METHOD FOR CFD APPLICATIONS

A. RAMEZANI* AND G. STIPCICH*

* BCAM - Basque Center for Applied Mathematics
Mazarredo 14, E48009 Bilbao, Basque Country, Spain
e-mail: gstipcich@bcamath.org, web page: <http://www.bcamath.org/>

Key words: Discontinuous method, High-order, Compressible, Euler equations, Finite volume

Abstract. The proposed method naturally merges the desirable conservative properties and intuitive physical formulation of the widely used finite-volume (FV) technique, with the capability of *local* arbitrary high-order accuracy and high-resolution which is distinctive in the *discontinuous* finite-element (FE) framework. This relatively novel scheme, the discontinuous hybrid control-volume/finite-element method (DCVFEM), has been already applied to the solution of advection-diffusion problems and shallow-water equations, and is in this paper extended to the Euler equations in the one-dimensional case. The main features are summarized and the scheme is compared to the well established FV and discontinuous Galerkin (DG) methods.

1 INTRODUCTION

In the framework of computational fluid dynamics (CFD) in engineering applications, low-order methods have been typically considered as the right choice due to their simplicity, robustness, and their effectiveness in providing a reasonably accurate solution by comparably low computational cost. Indeed the majority of the production and commercial codes are first or second order accurate. However, during the past two decades the interest in high order methods has grown not only among the research community, but also in the field of engineering, especially in certain applications where the complex flow structure and small length scales need to be adequately resolved. For instance, in wave propagation problems and in vortex dominated flows, the use of low-order methods may result in unacceptable solutions. In response to this trend, some high order algorithms have been proposed, such as tetrahedral *hp* finite elements [1], the spectral volume method [2], or the spectral method for the shallow water equations [3]. High order or *spectral* methods are usually referred to as methods of cubic convergence and above [4],

distinguishing from low-order methods, of the first and second order of convergence. Remaining in the field of CFD, the finite volume (FV), or control volume (CV), method is one of the most widely used techniques. Among the attractive features of the CV approach are quoted the excellent numerical conservation properties, the intuitive physical formulation and the relatively easy implementation.

Following the above considerations, in the present work is proposed an algorithm which incorporates the desirable physics-conserving properties of the CV method with the capability of arbitrary straightforward high order accuracy distinctive of the *discontinuous* finite-element (FE) approach, resulting in the hybrid discontinuous control-volume/finite-element method (DCVFEM hereafter). The formal derivation of the method has been provided in Stipcich et al. [5], along with a Fourier analysis in the one-dimensional case and convergence tests for the one- and two-dimensional cases for advection-diffusion problems.

Historically, the idea of combining the CV and FE method (CVFEM) arises from the instance of merging the inherent local numerical conservation property of the control volume method with the geometrical flexibility of the finite element method, resulting in the category of schemes also known as vertex- or node-based finite volume methods. The CVFEM can be seen as a finite-element method in which volume indicator distributions are used as weight functions [6]. The method has been developed originally by Baliga and Patankar [7] for advection-diffusion problems on triangular elements, where the integral conservation equations are enforced on polygonal control volumes constructed around each node of the mesh. The Poisson equation has been solved using quadrilateral elements [8] and successively advection-diffusion problems have been tackled [9]. The CVFEM has been further extended to incompressible flow using bilinear, quadrilateral elements and tetrahedral elements [10–13]. A detailed analysis of consistent and lumped versions of the CVFEM algorithm for diffusion-type problems has been carried out Banaszek [14], investigating the properties of bilinear, quadrilateral elements, nine-node (Lagrange) quadrilateral elements, eight-node Serendipity elements and six-node triangular elements. Some of the positive characteristics of the CVFEM approach are pointed out: local conservation is achieved at control volume level and the discrete maximum principle [15] is preserved. A high order CVFEM for unstructured grids was proposed by Piller and Stalio [16] for advection-diffusion problems, featuring a quadrature-free approach on quadrilateral elements. It is shown that an appropriate distribution of interpolation points and control-volume edges leads to a well conditioned matrix.

Discontinuous methods have been developed at first in the finite-element framework. The resulting discontinuous Galerkin methods (DGFEM), as opposed to the continuous Galerkin approach (GFEM), are characterized by the relaxation of the continuity constraint between neighboring elements, which is imposed in weak form through the so called *numerical fluxes* or *numerical traces* [17, 18]. The specific formulation of numerical fluxes strongly affects the consistency, stability and accuracy of the method [17]. The discontinuous philosophy has been applied within the CVFEM framework [3, 19], giv-

ing rise to discontinuous control volume/finite element methods. Research in this area has been mainly focused on hyperbolic problems [3, 19]. Iskandarani et al. [19] provide a thorough comparison of spectral GFEM, Taylor-Galerkin Least Square finite elements (TGLS), DGFEM and DCVFEM for the linear advection equation, using quadrilateral elements with interpolating polynomials of degree four to nine. The interpolation points within each element, in transformed space, are located at N Gauss-Legendre quadrature nodes while the control-volume edges lie on $N + 1$ Gauss-Lobatto-Legendre quadrature nodes.

The present work provides the extension of the spectral DCVFEM to the solution of the Euler equations in the one-dimensional case. The method is presented in its main features, and numerical experiments are conducted to verify the expected improved stability and accuracy in shock-capturing. The solution is compared to the well established DGFEM and FV method.

2 NUMERICAL APPROXIMATION

2.1 Governing equations

Although in the present work the one-dimensional case is considered, the mathematical derivation of the DCVFEM is presented in a general framework. The Euler equations in vector and conservative form read as

$$\frac{\partial \mathbf{U}}{\partial t} + \frac{\partial \mathbf{F}_i}{\partial x_i} = 0 \quad (1)$$

where the index $i = 1, 2, 3$ stays for the spatial dimensions of the problem, $x_i = \{x, y, z\}$ denotes the spatial coordinates, \mathbf{U} stands for the array of the conservative variables and $\mathbf{F}_i = \{\mathbf{F}_x, \mathbf{F}_y, \mathbf{F}_z\}$ are the vectors of flux quantities. In the one-dimensional case we have

$$\mathbf{U} = (\rho, \rho u, E_t)^T \quad \mathbf{F}_x = (\rho u, \rho u^2 + p, u(E_t + p))^T \quad (2)$$

where $t \in [0, \tau]$ represents time, ρ denotes the density, u the velocity, p is the pressure and E_t is the total energy per unit volume. System (1) is closed by the ideal gas law and complemented by suitable initial and boundary conditions.

2.2 Weak formulation

Considering a discretization (mesh) \mathcal{T}_h of $\bar{\Omega}$ into elements e , the discontinuous approximate solution can be defined as in [17]. The conservation equations (1) are multiplied by a test function ϕ and for each element e it is imposed the following

$$\int_e \frac{\partial \mathbf{U}}{\partial t} \phi \, d\mathbf{x} - \int_e \mathbf{F}_i \cdot \nabla \phi \, d\mathbf{x} + \int_{\partial e} \widehat{\mathbf{F}}_i \cdot \mathbf{n}_e \phi \, ds = 0 \quad (3)$$

where $\mathbf{x} \in \Omega$ is the position vector in the domain Ω , \mathbf{n}_e is the outward-pointing normal unit vector to the element and $\widehat{\mathbf{F}}_i$ is the appropriate *numerical flux*, *numerical trace*,

or Riemann solver. The definition of numerical traces is crucial, since it affects the consistency, stability and accuracy of the resulting discontinuous method [17].

The mesh \mathcal{T}_h is further subdivided into control volumes V , entirely contained in the respective element (see Figure 1). The weight function ϕ in (3) is chosen to be the volume indicator distribution, defined as

$$\phi \equiv \phi_V(\mathbf{x}) = \begin{cases} 1 & \text{if } \mathbf{x} \in V \\ 0 & \text{otherwise} \end{cases} \quad (4)$$

The weak formulation (3) then yields

$$\int_V \frac{\partial \mathbf{U}}{\partial t} d\mathbf{x} + \int_{\partial V} \mathbf{F}_i^- \cdot \mathbf{n} ds = \mathbf{0} \quad (5)$$

where \mathbf{n} denotes the outward-pointing normal unit vector to ∂V . By \mathbf{F}_i^- is denoted the trace on ∂V of the restriction of the flux quantities vectors \mathbf{F}_i to the volume V .

2.3 Coupling conditions: numerical fluxes

The surface integral appearing in (5) accounts for two different configurations for a control volume, according its intersection with the element's boundary ∂e being empty or not. The surface integral in (5) is calculated as

$$\int_{\partial V} \mathbf{F}_i^- \cdot \mathbf{n} ds = \left(\int_{\partial V \cap \dot{e}} \mathbf{F}_i \cdot \mathbf{n} ds + \int_{\partial V \cap \partial e} \widehat{\mathbf{F}}_i \cdot \mathbf{n} ds \right) \quad (6)$$

that is, on the faces of the control volume V that lay in the interior of the element \dot{e} the exact value of the flux quantities is used, whereas a suitably-defined numerical trace $\widehat{\mathbf{F}}_i$ is used for the faces laying on the boundary of the element ∂e . In the present work, a standard Roe's scheme [20] is enforced

$$\widehat{\mathbf{F}}_i = \{\mathbf{F}_i\} - \frac{1}{2}[\mathbf{A}][\widetilde{\mathbf{U}}] \quad (7)$$

where \mathbf{A} denotes the flux Jacobians, and the operators $\{\cdot\}$ and $[\cdot]$ are the inter-element average and jump:

$$\{\mathbf{F}_i\} \equiv \frac{1}{2}(\mathbf{F}_i^+ + \mathbf{F}_i^-) \quad [\mathbf{A}] \equiv \mathbf{A}^- - \mathbf{A}^+ \quad [\widetilde{\mathbf{U}}] \equiv \widetilde{\mathbf{U}}^- - \widetilde{\mathbf{U}}^+ \quad (8)$$

The above flux formulation (7, 8) must be limited to avoid destructive numerical oscillations near shocks. In the present work, the *generalized slope limiter* is used [17].

2.4 Finite dimensional subspace and basis functions

The unknowns $\mathbf{U}(\mathbf{x}, t)$ are approximated by element-based polynomial expansions [18]. The numerical approximations $\mathbf{U}_h(\mathbf{x}, t)$ are chosen in the same finite-dimensional subspace of $\mathbb{H}^1(\Omega)$ [21], spanned by a basis of piecewise polynomials L_j , defined in the transformed reference space $[-1, 1]^d$, which do not respect inter-element continuity. The choice $\mathbf{U}, \mathbf{F}_i \in \mathbb{H}^1(V)$ guarantees the existence of the integrals on V appearing in the weak formulation (5) [5]. In addition, a trace theorem asserts that a function in $\mathbb{H}^1(V)$ has a $\mathbb{L}^2(\partial V)$ trace [21, th. 1.3.1 ch. 1], assuring the existence of the boundary integrals appearing in (5).

In the present work, the Lagrange coefficients are chosen as piecewise (interpolatory) polynomials. For example, the restriction \mathbf{U}_h^e of \mathbf{U}_h to the element e is given by

$$\mathbf{U}_h^e \equiv \sum_{k=1}^{P^e+1} L_k \mathbf{U}_k^e \quad (9)$$

where $\{\mathbf{U}_k^e\}_{k=1}^{P^e+1}$ is the set of nodal values of \mathbf{U}_h in the element e and P^e denotes the polynomial order of the element. In principle, the interpolation nodes may be located everywhere inside an element, and in the present study the equally spaced placement is chosen.

2.5 Space discretization: subdivision into control volumes

Every element $e \in \mathcal{T}_h$ is further subdivided into control volumes V entirely contained in the element, i.e $V \subset e$. The subdivision into control volumes is a *dual partition* with respect to the original given discretization \mathcal{T}_h . This type of h -refinement [22] results in an increase of *local resolution* in the element e . In principle, any subdivision into control volumes V can be formed. In the present work, the equally spaced partition into control volumes is chosen. In Figure 1 is reported the sketch of the proposed subdivision for elements of order $P^e = 1, 2$. The procedure is general and straightforward for any polynomial order. For higher dimensions, the tensor product of the one-dimensional element can be used.

3 NUMERICAL EXPERIMENTS

The Euler equations are solved for a selected one-dimensional test case by the proposed DCVFEM and compared with the finite-volume (FV) and discontinuous Galerkin (DG) solutions.

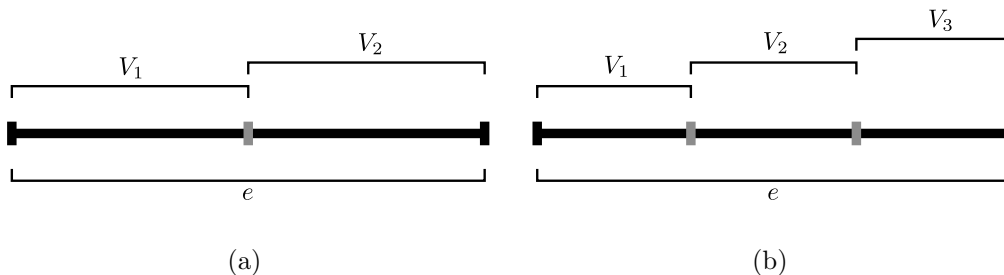


Figure 1: Sketch of the subdivision into control volumes V for a one-dimensional element e of polynomial order (a) $P^e = 1$ and (b) $P^e = 2$. The control volumes are entirely contained inside an element and the faces (represented by vertical solid color lines, black for external and gray for internal faces) are equally spaced.

3.1 Sod’s shock-tube problem

The shock-capturing capability of the DCVFEM is tested by the Sod shock-tube problem [23]. Equations (1, 2) are coupled with the following initial conditions

$$(\rho, u, p) = \begin{cases} (1, 0, 1) & t = 0, x \leq 0.5 \\ (0.125, 0, 0.1) & t = 0, x > 0.5 \end{cases} \quad (10)$$

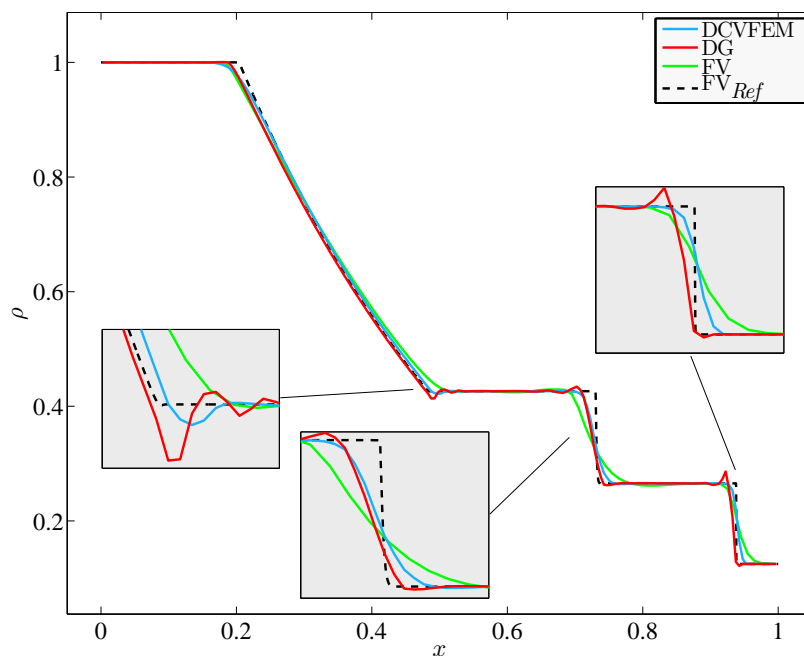
on the domain $x \in \Omega = [0, 1]$. The results for the density distribution are shown in Figure 2 (a), (b), (c) for different polynomial orders of accuracy $P^e = 1, 2, 3$, respectively. For the sake of comparison, the problem is also solved by the discontinuous Galerkin method (DG) using exactly the above described formulation for the inter-elements coupling and flux limiter (see Section 2.3). The solution is compared with the finite-volume (FV) method of second order accuracy for the case $P^e = 1$, since in this case the accuracy of the DCVFEM and DG are expected to be of second order as well. For the FV solution the symmetric minmod [24] flux limiter is used. All the presented simulations are run on a coarse mesh of 100 elements and by a fourth order Runge-Kutta time quadrature scheme. The chosen reference solution is the one obtained by the FV scheme on a very fine mesh of 10 000 elements, labeled as FV_{Ref} in the legend.

The following considerations are made:

- Figure 2 (a) shows the density distribution solution of *second order* accuracy (i.e. using polynomials of order $P^e = 1$ in DCVFEM and DG schemes) comparing the proposed DCVFEM with the DG and FV results on the same coarse mesh of 100 elements; it is observed that both the DCVFEM and DG exhibit better discontinuity-capturing capability and less dissipative behavior with respect to the FV in the expansion wave, in the contact discontinuity and in the shock; a certain amount of non-physical oscillations are observed in the DG solution in all discontinuity types,

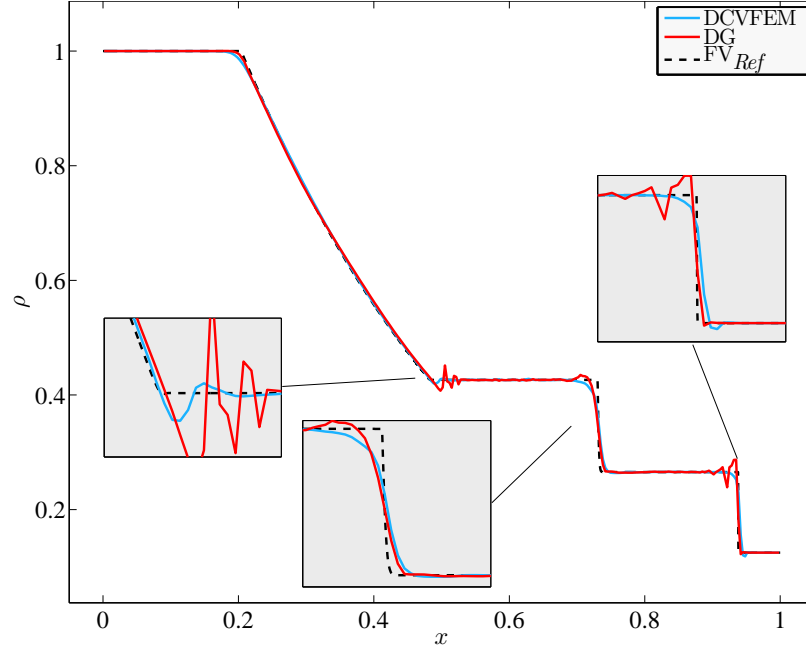
while some modest overshooting is exhibited by the DCVFEM in the expansion wave.

- Figure 2 (b) shows the density distribution solution of *third order* accuracy, i.e. using polynomials of order $P^e = 2$ by DCVFEM and DG schemes, on the same coarse mesh of 100 elements; both schemes exhibit a comparable discontinuity-capturing capability in the rarefaction wave, contact discontinuity and in the shock; however, the DCVFEM solution is free from visible numerical oscillations and overshooting, while the DG solution is affected by rather severe oscillations near the discontinuities.
- Figure 2 (c) shows the density distribution solution of *fourth order* accuracy, i.e. using polynomials of order $P^e = 3$ by DCVFEM (the DG scheme is not converging in this case) on the coarse mesh of 100 elements; the solution by the proposed DCVFEM exhibits an overall better shock-capturing capability, as expected when using a higher-order accuracy; no visible numerical oscillations are observed, except some modest overshooting in the expansion wave.

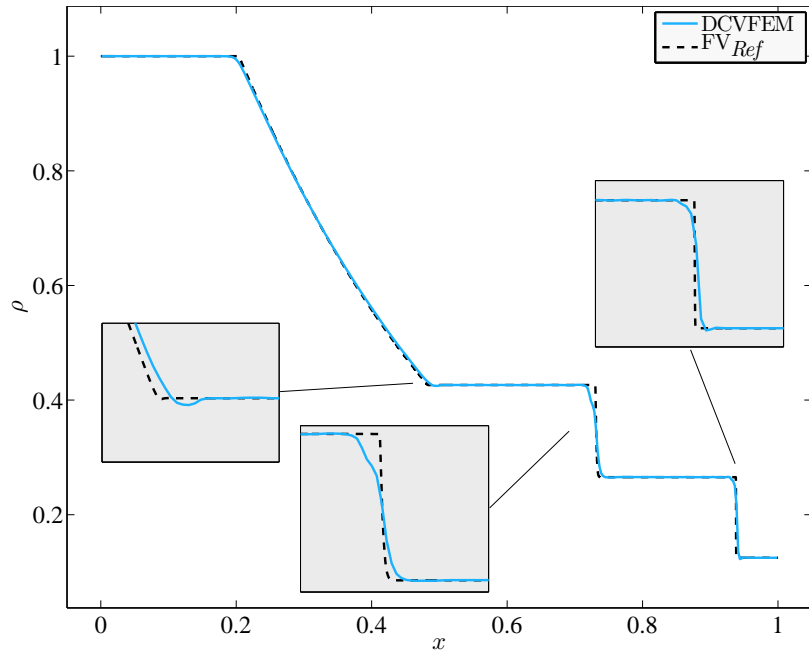


(a) Second order accuracy solution (i.e. polynomial order $P^e = 1$)

Figure 2: Density distribution for the shock-tube problem (10) on a coarse mesh of 100 elements for (a) $P^e = 1$, (b) $P^e = 2$ and (c) $P^e = 3$.



(b) Third order accuracy solution (i.e. polynomial order $P^e = 2$)



(c) Fourth order accuracy solution (i.e. polynomial order $P^e = 3$)

4 CONCLUSIONS

The high-order discontinuous hybrid control-volume/finite-element method (DCVFEM) has been successfully applied to the solution of the Euler equations in the one-dimensional case. The derivation for the general multi-dimensional case has been reported and the main features of the proposed scheme have been described. The DCVFEM solution of the shock-tube test case has been compared with the well established discontinuous Galerkin (DG) scheme by using the same inter-element coupling formulation and flux limiter, and with the classical finite-volume (FV) method for the second order accuracy. The DCVFEM solution appears to be more accurate and less dissipative than the FV, and does not present visible unphysical oscillations which instead affect considerably the DG solution. This desirable advantage of the DCVFEM is most likely related to the weak formulation of the scheme, which is proven to be conservative at *control volume* level [5], differently from the DG formulation, which features conservation at element level. Nevertheless, the scheme is seen to be very sensitive to the particular choice of the flux limiter formulation, which demands additional analysis and experimentation. The numerical results reported in the present one-dimensional study are encouraging for the further extension of the DCVFEM to the multidimensional case of the Euler equations.

REFERENCES

- [1] S. J. Sherwin and G. E. Karniadakis. Tetrahedral hp finite elements: algorithms and flow simulations. *Journal of Computational Physics*, 124(1):14 – 45, 1996. ISSN 0021-9991.
- [2] Z. J. Wang. Spectral (finite) volume method for conservation laws on unstructured grids: basic formulation. *Journal of Computational Physics*, 178:210–251, 2002.
- [3] B. J. Choi, M. Iskandarani, J. C. Levin, and D. B. Haidvogel. A spectral finite volume method for the shallow water equation. *Monthly Weather Review*, 132(7):1777–1791, 2004.
- [4] Z.J. Wang, Krzysztof Fidkowski, Rémi Abgrall, Francesco Bassi, Doru Caraeni, Andrew Cary, Herman Deconinck, Ralf Hartmann, Koen Hillewaert, H.T. Huynh, Norbert Kroll, Georg May, Per-Olof Persson, Bram van Leer, and Miguel Visbal. High-order cfd methods: current status and perspective. *International Journal for Numerical Methods in Fluids*, 72(8):811–845, 2013.
- [5] G. Stipcich, M. Piller, M. Pivetta, and L. Zovatto. Discontinuous control-volume/finite-element method for advectiondiffusion problems. *Computers & Fluids*, 52(0):33–49, 2011. ISSN 0045-7930.
- [6] M. J. Martinez. Comparison of Galerkin and control volume finite element for

- advection-diffusion problems. *International Journal for Numerical Methods in Fluids*, 50:347–376, 2006.
- [7] B. R. Baliga and S. V. Patankar. A new finite-element formulation for convection-diffusion problems. *Numerical Heat Transfer, Part B: Fundamentals*, 3(4):393–409, 1980.
- [8] S. Ramadhyani and S. V. Patankar. Solution of the poisson equation: Comparison of the galerkin and control-volume methods. *International Journal for Numerical Methods in Engineering*, 15(9):1395–1402, 1980. ISSN 1097-0207.
- [9] S. Ramadhyani and S. V. Patankar. Solution of the convection-diffusion equation by a finite-element method using quadrilateral elements. *Numerical Heat Transfer Part B-fundamentals*, 8:595–612, 1985.
- [10] G. E. Schneider and M. J. Raw. A skewed, positive influence coefficient upwinding procedure for control-volume-based finite-element convection-diffusion computation. *Numerical Heat Transfer, Part B: Fundamentals*, 9(1):1–26, 1986.
- [11] C. Masson, H. J. Saabas, and B. R. Baliga. Co-located equal-order control-volume finite element method for two-dimensional axisymmetric incompressible fluid flow. *International Journal for Numerical Methods in Fluids*, 18:1–26, 1994.
- [12] H. J. Saabas and B. R. Baliga. Co-located equal-order control-volume finite-element method for multidimensional, incompressible fluid flow—part I: formulation. *Numerical Heat Transfer, Part B: Fundamentals*, 26(4):381–407, 1994.
- [13] H. J. Saabas and B. R. Baliga. Co-located equal-order control-volume finite-element method for multidimensional, incompressible fluid flow—part II: verification. *Numerical Heat Transfer, Part B: Fundamentals*, 26(4):409–424, 1994.
- [14] J. Banaszek. Comparison of control volume and Galerkin finite element methods for diffusion-type problems. *Numerical Heat Transfer, Part B: Fundamentals*, 16(1): 59–78, 1989.
- [15] P. C. Ciarlet. Discrete maximum principle for finite difference operators. *Aequationes Mathematicae*, 38:1676–1706, 2000.
- [16] M. Piller and E. Stalio. Development of a mixed control volume - finite element method for the advection–diffusion equation with spectral convergence. *Computers & Fluids*, 40(1):269–279, 2011.
- [17] B. Cockburn. Discontinuous Galerkin methods. *Journal of Applied Mathematics and Mechanics*, 11:731–754, 2003.

- [18] B. Q. Li. *Discontinuous finite elements in fluid dynamics and heat transfer*. Springer-Verlag, Berlin, 2006.
- [19] M. Iskandarani, J. C. Levin, B. J. Choi, and D. B. Haidvogel. Comparison of advection schemes for high-order h-p finite element and finite volume methods. *Ocean Modeling*, 10:233–252, 2004.
- [20] P. L. Roe. Approximate Riemann solvers, parameter vectors, and difference schemes. *Journal of Computational Physics*, 43(2):357–372, 1981.
- [21] A. Quarteroni and A. Valli. *Numerical approximation of partial differential equations*. Springer-Verlag Italia, Milano, 1994.
- [22] G. E. Karniadakis and S. J. Sherwin. *Spectral/hp element methods for CFD*. Oxford University Press, Oxford, 2005.
- [23] G. A. Sod. A survey of several finite difference methods for systems on non-linear hyperbolic conservation laws. *Journal of Computational Physics*, 27(1):1–31, 1978.
- [24] P. L. Roe. Characteristic-based schemes for the euler equations. *Annual Review of Fluid Mechanics*, 18(1):337–365, 1986.